Approximate Solutions to Some Problems in Polyelectrolyte Theory Involving Nonuniform Charge Distributions

Gerald S. Manning†

Department of Chemistry and Chemical Biology, Rutgers University, 610 Taylor Road, Piscataway, New Jersey 08854-8087

Received March 20, 2008; Revised Manuscript Received May 22, 2008

ABSTRACT: We give approximate solutions for some problems in polyelectrolyte theory involving nonuniform charge distributions. Distributions of condensed counterions and electrostatic free energies are found for line-charge models of oligomers, end segments, junctions separating regions of different charge densities, and two semi-infinite line charges approaching each other end-on. The end-on potential of mean force in the latter case is screened by the Debye length. With that exception, we find little correlation between the Debye screening length and the much smaller distances marking the onset of significant end effects. We suggest a biological application to DNA unwinding by helicases.

I. Introduction

A useful line of research in the development of polyelectrolye solution theory has centered on the model of an infinitely long line of discrete charge sites with uniform spacing.[1–6] The infinite length does not detract from the realism of the model in predicting a variety of polyelectrolyte properties dependent on interactions between the polyion and its surrounding distribution of neutralizing ions, since the two ends at $\pm\infty$ are screened from each other by the small ions. A dominant consequence of the asymptotically logarithmic electrostatics of the line charge is counterion condensation. Above a critical line charge density, exactly enough counterions condense on the line to reduce its effective charge to the critical value, regardless of polymer (hence counterion) concentration or of ionic strength set by addition of bulk salt.

For a stiff polyion like DNA, the line can represent the central axis of the double helix, and the charge sites become average positions of the negatively charged phosphate groups when projected onto this axis. Although important consequences of the helical charge arrangement are thereby missed, still the line model captures aspects of DNA ionic behavior that are dominated by long-range electrostatics.[6] In particular, the prediction that the effective charge on DNA after condensation of univalent counterions is equal to 0.48 e^- per base pair (there are two phosphates per base pair) is in close agreement with the value 0.50 ± 0.05 directly extracted from electrical force measurements on a single DNA molecule independent of salt concentration over the range explored, 0.02−1 M KCl.[7] A supplementary measurement in 0.2 M NaCl yielded the same value.[7]

The theoretically predicted threshold charge density for condensation of counterions depends on the valence of the counterion; counterions of higher valence condense at lower thresholds. Values directly observed in ion-exchange diffusion data for condensation of univalent, divalent, and trivalent counterions on relatively stiff polysaccharides conform closely to the predicted values.[8]

Thermodynamic signatures of counterion condensation are strongly depressed and concentration-independent activity-to-concentration ratios (activity coefficients) and pressure-to-concentration ratios (osmotic coefficients), such as has been observed in solutions of univalent counterions and a synthetic polycation engineered for stiffness.[9] For DNA, the theory of condensation of divalent counterions on a line charge is in close agreement with measured Mg^{2+} ion activity coefficients.[1]

The line charge model is of course incapable of describing the chain statistics of flexible charged polymers. Nonetheless, the relevant length scale for polyion−small ion interactions is on the order of a Debye length $1/\kappa$, and on this scale a charged flexible polymer segment is probably more or less straightened by the charge−charge repulsions. Structure functions from scattering data on semidilute solutions of a synthetic polymer with varying charge density on a flexible hydrophilic backbone have confirmed threshold counterion condensation.[10] In dilute solutions, the same system yielded concentration-independent osmotic coefficients in close agreement with predicted values.[11] Measurements of the related Donnan salt exclusion coefficient gave similar results.[12,13] Osmotic pressures and metal ion activity coefficients in solutions of flexible chains with a wide variety of divalent metal counterions revealed the thermodynamic signature of condensation and close agreement with predicted values.[14–16] Hydrophobic flexible backbones do not exhibit deviation from expected counterion condensation behavior as long as the density of charged groups along the backbone is high.[11] Hydrophobic backbones with relatively low charge densities (but still above the condensation threshold) do deviate from canonical behavior, as discussed by Essafi et al.[11]

There is a class of problems that cannot be addressed by the infinite line of uniformly distributed discrete charge sites. Counterion condensation on an oligomeric chain shorter than $1/\kappa$ is one such problem. Condensation at the end of a long polymer is another. In both cases, the uniform charge density on the polymer abruptly meets a region of zero charge density, and the electrostatic behavior is determined by the nonuniformity across the interface. In block copolymers, it is possible to have a junction between two regions of nonzero but different charge site densities, thus providing a third example. Still another example would be two identically charged segments, aligned end-on but with a gap between them.

In the context of cell biology, a nonuniform charge distribution may be an important aspect of the environment of proteins that unwind the two strands of double-helical DNA, such as the family of helicases. The helicase machine tracks along a single DNA strand, separating the two strands of the double helix ahead of it and thus creating a fork where separated strands merge into the double helix.[17] There is a strongly nonuniform DNA phosphate charge distribution at the fork, and the proteins bear ionized groups as well. An issue is whether the unwinding

†E-mail: jerrymanning@rcn.com.

10.1021/ma800628v CCC: $40.75
Published on Web 07/22/2008

mechanism is passive, whereby the protein waits for a thermal strand-opening fluctuation before progressing into the fork, or whether the protein actively assists in opening the double helix.[18] There is evidence that some helicases act to open the double helix,[19] and then the question arises of how much electrostatic interactions may contribute to the energetics of the opening mechanism.[19]

There has been some theoretical and computational work on oligomers and end segments.[20–28] It might be thought that condensation of counterions on an oligomer shorter than a Debye length does not occur, but it does, because even in this case a supercritical charge on an extended oligomer competes effectively with the entropy of counterion dissociation.[21,24,25] It might also be thought that there would be a progressive falloff of the number of counterions condensed near the end of a long polymer, beginning at a distance of the order of $1/\kappa$, but the tenaciousness of the concentration of counterions at the surface of a charged cylinder up to its very end is a striking feature of the simulations reported by Washizu and Kikuchi.[27] In the present paper we use a finite-length variant of the line-of-discrete charges model to arrive at approximate evaluations of the number of counterions condensed on oligomers, end segments, junctions, and two disjoint segments with a gap between them, and we also estimate the electrostatic free energies of these objects. The free energy of the disjoint segments provides a route for calculating the potential of mean force for the end-on approach of two rodlike polymers. An automatic bonus is the electrostatic closure free energy for connecting two rods into a single rod, which in turn contributes to the closure of a rod into a ring, as first understood and analyzed by Kunze and Netz.[28] Finally, we suggest applications to the active mechanism engaged by some DNA unwinding machines.

II. The System and Its Length Scales

The polymers, polymer segments, and oligomers are modeled as collections of unit charges $\pm e$, all with the same sign, held at fixed positions. These charge assemblies (with their mobile counterions) are immersed in a medium (solvent) with dielectric constant D (dimensionless). For pure water at room temperature, $D = 78.5$, but for any polar solvent, especially water, the dielectric "constant" is a strongly decreasing function of temperature, $\epsilon = \epsilon(T)$. If the medium is aqueous $z{:}z'$ electrolyte (salt), then D also depends on salt concentration.

The notation and units for the electrolyte are conventional. If its formula is $A_\nu B_{\nu'}$, then the respective unsigned valences z and z' are such that the formula is electrically neutral, $\nu z = \nu' z'$. As an example, for the Na^+ cation and the SO_4^{2-} anion, the neutral salt is Na_2SO_4, a 1:2 electrolyte. The defining formula for the ionic strength I of an electrolyte solution consisting of a single salt fully dissociated in the solvent is $I = (1/2)(cz^2 + c'z'^2)$, which may be rewritten as $I = (1/2)c_s z z'(\nu + \nu')$, where c and c' are the respective concentrations of the ions and c_s is that of the salt. The units of ionic and salt concentrations, and thus of ionic strength, are molarity M (mol/L). Notice that $I = c_s$ for a 1:1 salt solution.

The Debye screening length of the electrolyte solution is $1/\kappa$, where the square of the inverse of this length is defined by the formula $\kappa^2 = 8000\pi N_A l_B I$, where N_A is Avogadro's number and $l_B = e^2/4\pi D\epsilon_0 k_B T$ is the Bjerrum length (ϵ_0 is the permittivity of free space and k_B is the Boltzmann constant). The physical significance of the Bjerrum length is that it is the distance between two unit charges at which the Coulomb's law free energy (D is temperature dependent) equals $k_B T$.

The units in this formulation of the definition of κ^2 are mixed since, as mentioned, the ionic strength I is in molarity (M). The formula then yields the Debye length $1/\kappa$ in meters (m) if the Bjerrum length is calculated in meters. A convenient numerical formula, valid in water at room temperature (where $l_B = 0.71$ nm), is $1/\kappa = 0.305 I^{-1/2}$ nm. At "physiological" ionic strength 0.1 M, the Debye screening length equals 0.96 nm in these conditions.

As for the fixed charge assemblies themselves, all of them in this paper will incorporate, at least, subcollections of charged sites arranged linearly with uniform spacing b. A convenient dimensionless measure of the charge density $1/b$ is the ratio $\xi = l_B/b$. For double-helical DNA in its canonical B structure, $b = 0.17$ nm (two phosphates per 0.34 nm rise from one base pair to the next) and $\xi = 4.2$ in water at room temperature.

An important quantity in the following development is the internal partition function Q of the condensed counterions. Because salt concentrations are in molarity units, the units of Q turn out as liters per mole of fixed charges. For a long B-form DNA, $Q = 0.641$ L/(mol phosphate) for univalent counterions. To get a qualitative feeling for the meaning of this number, we have pointed out that if Q is roughly modeled as a free volume for the condensed counterions, it would correspond to a cylindrical shell around the DNA molecule of thickness 0.7 nm.[1]

As a final but important observation, our intention in this paper is to analyze charge assemblies that have linear dimensions less than a Debye length. The Coulomb interaction between any two fixed charge sites in the assembly are therefore taken as unscreened by small ions (the single exception is in section VI and will be noted explicitly).

III. Oligomers

In this section we consider P charge sites arranged on a line with spacing b. The oligomer is short (or the electrolyte is dilute), such that the oligomer length $L = (P - 1)b$ is considerably less than a Debye length $1/\kappa$. On the other hand, we assume that P greatly exceeds unity, which can thus be neglected in comparison to P. We then have the ranking $1 \ll P \ll 1/(\kappa b)$, or for the lengths, equivalently, $b \ll L \ll 1/\kappa$. However, for purposes of numerical comparison of mathematical theory to physical data, we will not hesitate to apply our results in a physical environment of less restrictive conditions $b < L < 1/\kappa$.

Because of the possibility of counterion condensation, the effective charge at each site may be less than its unit value. The effective charge fraction is denoted by f, and $f = 1 - z\theta$, where θP is the number of counterions of valence z condensed on the oligomer. Thus, f in the following equations is a function of θ, and $df/d\theta = -z$. Notice that we are assuming uniform counterion condensation along the length of the oligomer. The expectation is that there will turn out to be less condensation on the oligomer than on the corresponding long polymer, and it is quantification of this "oligomer effect" that we wish to emphasize, not intraoligomer variations. We recognize that an improved theory might be able to handle the symmetrical rise of condensed counterion density from both ends of the oligomer toward a maximum in the middle more accurately.

In writing an expression for the Coulomb free energy of interaction among oligomer charge sites, we do not use an exponential screening factor, since any two of the sites are separated by a distance less than a Debye screening length. We use g to denote free energy in $k_B T$ units. Then for the Coulomb interaction free energy

$$g_{\text{coulomb}} = \xi f^2\left[(P-1) + \frac{1}{2}(P-2) + \frac{1}{3}(P-3) + \ldots\right] \quad (1)$$

where the series cuts off after $P - 1$ terms. The first term of the series represents the $P - 1$ nearest-neighbor interactions, the second the $P - 2$ next-nearest-neighbor interactions, and so on. We can evaluate this expression to leading order in large P by replacing $(P - n)$ with P and then realizing that the

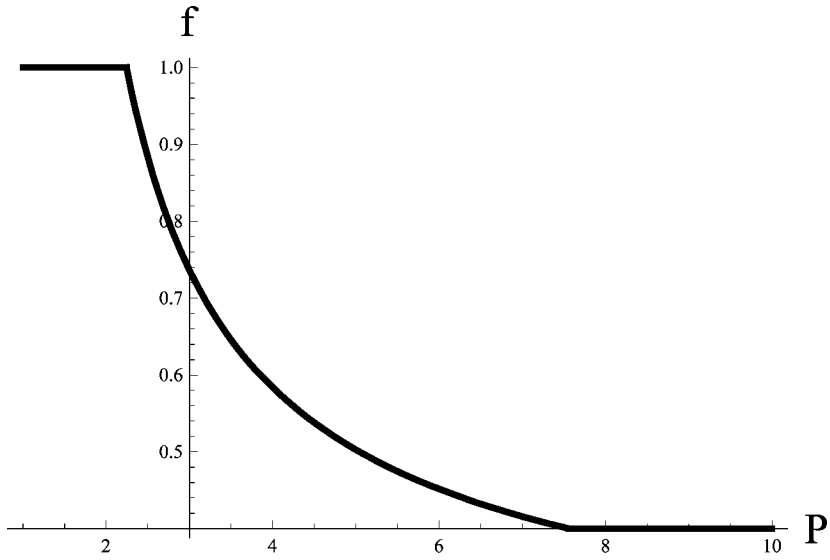

Figure 1. Plot of charge fraction f per site on an oligomer with P charge sites and univalent counterions. The numerical values of the parameters in eqs 8 and 9 are $\xi = 2.5$ ($b = 0.28$ nm) and $1/\kappa = 2.15$ nm (ionic strength = 20 mM).

harmonic series that results after factoring out P is asymptotic to ln P. To leading order

$$g_{\text{coulomb}} = \xi f^2 P \ln P \tag{2}$$

The Coulomb free energy is not the only contribution to the overall electrostatic free energy. There is also a free energy associated with the transfer of the θP condensed counterions from bulk to the condensed layer

$$g_{\text{transfer}} = \theta P \ln \frac{\theta}{\gamma \nu c_s Q} \tag{3}$$

In this formula νc_s is the bulk counterion concentration, γ is an activity coefficient in bulk, and Q is the internal partition function for the condensed counterions (assumed to be independent of θ). Since c_s is bulk salt molarity and $\theta P/N_A$ is the number of moles of counterions condensed on the oligomer, QP/N_A must have liter units, and as stated in the previous section, Q then has the units liters per mole of fixed charge sites.

The overall electrostatic free energy of the oligomer is the sum of the two components:

$$g_{\text{el}} = g_{\text{coulomb}} + g_{\text{transfer}} \tag{4}$$

In writing out the formula for it, we have found it convenient to use the square of the Debye parameter κ^2 instead of salt concentration c_s. With reference to section II, we get

$$g_{\text{el}} = \xi f^2 P \ln P - 2\theta P \ln \kappa b + \theta P \ln(\theta a l_B b^2/Q) \tag{5}$$

where the constant a is given by

$$a = 4000\pi N_A z z' (\nu + \nu')/\gamma\nu \tag{6}$$

In the expression for g_{el} there are two unknowns: the fractional number θ of condensed counterions (and along with it, $f = 1 - z\theta$) and the condensed counterion partition function Q. To determine equilibrium values, we begin by setting $\partial g_{\text{el}}/\partial\theta$ equal to zero

$$2z\xi f \ln P + 2 \ln \kappa b - \ln(\theta a l_B b^2 \mathbf{e}/Q) = 0 \tag{7}$$

where **e** in the third term is the base of logarithms. Asymptotically, the first two terms dominate, since both P and $1/\kappa b$ are large quantities. Therefore, the sum of the first two terms may be set equal to zero independently of the third term, thus producing a trivially solvable equation in the single unknown f

$$f = \xi_{\text{crit}}/\xi \tag{8}$$

where

$$\xi_{\text{crit}} = -\frac{\ln \kappa b}{z \ln P} \tag{9}$$

This formula yields meaningful values of f, namely $f < 1$, as long as the bare charge density parameter ξ of the oligomer exceeds a critical value ξ_{crit}. Then sufficiently many counterions condense on the oligomer to reduce the bare charge density ξ to an effective value ξ_{crit}. Notice that when the bare number of oligomer charges P equals $1/\kappa b$, that is, when the oligomer length Pb is equal to the Debye screening length $1/\kappa$, its maximum value for validity of the formula, then $\xi_{\text{crit}} = 1/z$, the value for a long polymer, and $f = 1/z\xi$. The value of P less than which counterions do not condense is obtained by setting $f = 1$ in eq 8 and then solving for this value of P using eq 9.

Ramanathan was the first to derive this expression for the oligomer charge fraction, using a more intricate analysis.[21] Here it is derived in the same way as in Mohanty and Manning[24] but as part of a broader program that emphasizes the electrostatic free energy. Netz has derived a similar formula to describe the zero-field coupling between explicit counterions and flexible chains in his simulations of polyelectrolytes in external electric fields.[25]

We give a numerical illustration in Figure 1 for structural parameters and concentrations corresponding to the system of polystyrenesulfonate oligomers with univalent counterions used by Cottet et al. in their mobility study.[29] Oligomer lengths up to eight charged sites are shorter than a screening length in these conditions. We predict the onset of significant counterion condensation, such that the effective oligomer charge fraction f per site is decreased from its bare value of unity, at a remarkably small number of oligomer charges.

The dependence of the effective charge fraction on the number of oligomer charges is qualitatively similar to that found in the simulations of Frank and Winkler,[26] who present a plot of $1 - f$ (fraction of condensed counterions) against oligomer charge number, using similar structural parameters but different ionic conditions, including application of a weak field to simulate oligomer mobility. Both results suggest that significant

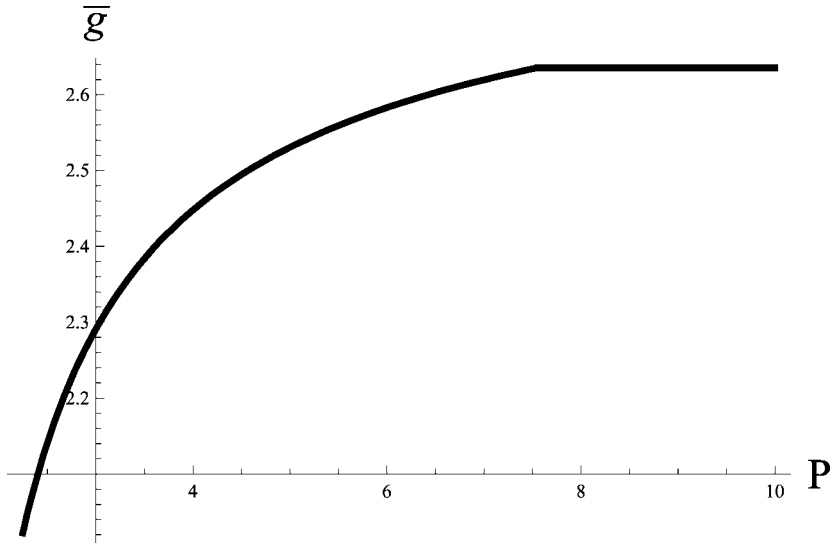

Figure 2. Plot of the electrostatic free energy $\bar{g}_{el}$ per charge site in units of k_BT for an oligomer with P charge sites. The numerical values of the parameters in eq 11 are given in the caption to Figure 1.

condensation begins at a small number of oligomer charges, followed by a progressive increase in the number of condensed counterions up to the polymer plateau at oligomer lengths that are still not very long. Although quantitative comparison is not possible, the simulation suggests that our formula may quantitatively overestimate the extent of condensation, yielding a value for the condensation fraction at oligomer charge number $P = 10$ about equal to 0.2, whereas Figure 1 would indicate the larger value 0.6 at $P = 8$. On the other hand, the value 0.74 for the condensation fraction found by Netz[25] in a zero-field simulation for a longer chain, $P = 50$, of linear charge density similar to a 25 base pair DNA oligomer, in ionic conditions such that the length of this chain equals a Debye screening length, compares favorably with our calculated condensation fraction 0.80 (and also with Netz's calculated value 0.70 from his similar formula).

We focus next on the internal partition function Q of the condensed layer of counterions. We found f by setting the first two terms of the equilibrium condition eq 7 independently to zero, since they dominate the left-hand side. Now we set the third term to zero in order to satisfy the condition to a higher order. The argument of the logarithm in this term being then equal to unity, we get

$$Q = \theta a l_B b^2 \mathbf{e} \tag{10}$$

where θ at this point is the equilibrium value $z^{-1}(1 - f)$, f from eq 8. This formula should be interpreted as a consistency condition on Q. Although in a very simple model, Q can be regarded as a local free volume for the condensed counterions,[1] in general it is a complicated affair involving interactions between a condensed counterion and the solvated polymer structure. But no matter how complicated may be the various components of Q, they must mutually adjust such that the overall value of the condensed layer partition function is consistent with the long-range electrostatics of the system as expressed by eq 10.

For present purposes the most interesting information contained in eq 10 emerges immediately on noticing that the ratio $Q/Q_\infty = \theta/\theta_\infty$, where the subscripts refer to a long polymer. Since, per charge site, the number of counterions condensed on the oligomer is less than on the polymer, it follows that the partition function, per charge site, of the counterion layer condensed on the oligomer is less than it is on the polymer. The oligomeric condensed layer is less stable than the polymeric condensed layer.

With f and Q in hand, we can calculate the electrostatic free energy (k_BT units) of an oligomer with P charge sites as expressed by eq 5

$$\bar{g}_{el}(P) = \xi[f(P)]^2 \ln P - z^{-1}[1 - f(P)] \ln(\mathbf{e}\kappa^2 b^2) \tag{11}$$

where the overbar means "per oligomer charge", $\bar{g}_{el} = g_{el}/P$. It may be verified that this formula becomes identical to eq 7 of ref 5 for the polymer free energy per charge when P is replaced by its maximum value $1/\kappa b$. Notice that the activity coefficient γ of bulk counterions has canceled out. Figure 2 illustrates how the electrostatic free energy per oligomer charge increases with oligomer length to the corresponding polymer plateau.

IV. End Segments

As in section III we again consider unit charge sites 1,..., P laid out on a line with spacing b. But in contrast to the preceding section, where there were no charge sites either to the left of site 1 or to the right of site P, here there are charge sites $P + 1$,..., ∞ that represent the interior of a polymer. In other words, here the first P sites are either at (namely, site 1) or near (sites 2,..., P) the end of a long polymer. The expectation is that the number of counterions condensed at the end of the polymer is minimal and then increases with distance toward the polymer interior until it reaches a plateau at the constant value in the polymer interior.

Odijk[23] formulated an equilibrated local chemical potential model to study counterion condensation on an end segment of a linear charged micelle. He concluded that end effects are manifested within a distance $1/\kappa$ from the end. Manning and Mohanty[24] also used this method to arrive at an expression for the critical charge density of a continuous line charge as a function of distance into the line from its end. They also concluded that an end segment has length $\sim 1/\kappa$. The simulations of Washizu and Kikuchi[25] confirm the Debye length as the scale of end effects, but a striking result of the simulations is that the concentration of counterions at the surface of a charged cylinder (with DNA parameters) falls off only slightly until close to the actual end of the cylinder. In this section we improve the estimate of Manning and Mohanty within the context of an extended treatment that also allows calculation of the electro-

static free energy density as a function of distance from the end toward the interior.

We begin by writing an expression for the Coulomb free energy of interaction among the P charge sites in the end segment. We assume that the length $(P-1)b$ of the end segment is equal to $1/\kappa$. The interactions are therefore taken as unscreened. In k_BT units

$$g_{\text{coulomb}} = \xi \sum_{n=1}^{P-1} \sum_{m=1}^{P-n} f_m f_{m+n}/n \tag{12}$$

where f_l is the effective charge fraction at site l, $f_l = 1 - z\theta_l$, and $z\theta_l$ is the fractional charge of counterions condensed at site l, $l = 1...P$. For example, for the fixed value $n = 2$, the inner sum gives the Coulomb's law interaction between effective charges within the end segment separated by distance $2b$. We consider interactions between sites in the end segment and sites $P+1,...\infty$ as screened and therefore negligible. The free energy associated with transfer of counterions from bulk to the layer condensed on the end segment is

$$g_{\text{transfer}} = \sum_{i=1}^{P} \theta_i \ln \frac{\theta_i}{\gamma \nu c_s Q_i} \tag{13}$$

where Q_i is the internal partition function of the counterions condensed at site i (in a simple model, θ_i/Q_i is a local density of counterions condensed at site i). The total electrostatic free energy g_{el} of the end segment is the sum of these two components.

To determine the condensed fractions at the various sites, we need partial derivatives with respect to θ_l, $l = 1...P$

$$\frac{\partial g_{\text{coulomb}}}{\partial \theta_l} = -z\xi\left[(f_{l-1} + f_{l+1}) + \frac{1}{2}(f_{l-2} + f_{l+2}) + \cdots \frac{1}{l-1}(f_1 + f_{2l-1})\right] - z\xi\left[\frac{1}{l}\left(f_{2l} + \frac{1}{l+1} f_{2l}\right) + \cdots \frac{1}{P-1} f_P\right] \tag{14}$$

We have delineated two distinct classes of terms, $\mathscr{A}$ and $\mathscr{B}$, by the two sets of brackets. The class $\mathscr{A}$ terms represent pairwise interactions between site l and the $l-1$ sites to its left, down to the end site 1, as well as the symmetrical interactions with the $l-1$ sites to its right. Class $\mathscr{B}$ terms reflect interactions of site l with sites still further to its right, but still within the end segment. Let us note at the outset that if we were to consider only class $\mathscr{A}$ interactions, we would arrive exactly at the Manning and Mohanty result.[24] The result we will obtain here, since it considers more of the existing interactions, must be an improvement over the Manning and Mohanty calculation.

We handle the two classes of interactions with different asymptotic approximations. We consider site l as lying deep in the interior of the end segment; l is a large number. Therefore, $l - i \sim l$ for most of the class $\mathscr{A}$ terms, and $f_{l-i} \sim f_l$ for class $\mathscr{A}$. The class $\mathscr{B}$ interactions are between site l and sites distant from it toward the interior of the polymer. For these interactions, we set $f_i \sim 1/z\xi$, the constant plateau value for interior sites. With these approximations, we have

$$\frac{\partial g_{\text{coulomb}}}{\partial \theta_l} = -2z\xi f_l\left(1 + \frac{1}{2} + \cdots \frac{1}{l-1}\right) - \left(\frac{1}{l} + \frac{1}{l+1} + \cdots \frac{1}{P-l}\right) \tag{15}$$

We pass next to a continuous description, which involves replacing the sums by integrals, the recognition that the distance s in from the end equals $(l-1)b$, and that l, hence s, is in the interior of the end segment, $b \ll s \ll (P-1)b = 1/\kappa$. Switching to the standard notation for a variational derivative, we get

$$\frac{\delta g_{\text{coulomb}}}{\delta \theta(s)} = [1 - 2z\xi f(s)] \ln\left(\frac{s}{b}\right) + \ln \kappa b \tag{16}$$

The variation of g_{transfer} is more easily accomplished, since the ith term of the sum in eq 13 depends only on the value of θ at site i. Then

$$\frac{\delta g_{\text{transfer}}}{\delta \theta(s)} = \ln\left[\frac{\theta(s) a l_B b^2 \mathbf{e}}{Q(s)}\right] - 2 \ln \kappa b \tag{17}$$

The equilibrium condition is that the variation of g_{coulomb} equal the negative of the variation of g_{transfer}. It is

$$[1 - 2z\xi f(s)] \ln\left(\frac{s}{b}\right) - \ln \kappa b + \ln\left[\frac{\theta(s) a l_B b^2 \mathbf{e}}{Q(s)}\right] = 0 \tag{18}$$

The first two logarithmic terms dominate the left-hand side and must be independently set to zero, yielding a formula for the equilibrium value of the effective charge fraction $f(s)$ along the length of the end segment

$$f(s) = \frac{1}{2z\xi}\left(1 - \frac{\ln \kappa b}{\ln s/b}\right) \tag{19}$$

Notice that when $s = 1/\kappa$, which defines the boundary between the end segment and the interior of the polyelectrolyte, $f(s)$ takes the value $1/z\xi$, the constant charge fraction in the interior.

In Figure 3 we show plots of the fractional number of condensed counterions $\theta = z^{-1}(1 - f)$ as a function of distance from the end of the polymer normalized to a Debye length, $s/\kappa^{-1} = \kappa s$. We see behavior like that reported by Washizu and Kikuchi,[27] especially for the lower ionic strength. The end effect is small. The uniform interior value of θ extends toward the end (to the left in the figure) well past a Debye screening distance and falls steeply to zero only very near the end itself. The length s_0 of the segment on which no counterions are condensed, measured from the end, is obtained by setting $f(s_0) = 1$ in eq 19

$$s_0 = b(\kappa b)^{1/(1-2z\xi)} \tag{20}$$

This length may not have the same universal character as the persistence length of the polymer, the Bjerrum length, or the Debye length, but it is of interest since it appears to be a more accurate measure of the scale of end effects than the Debye length. It serves once again to emphasize that important polyelectrolyte effects are a consequence of nonlinear electrostatics.

Setting the higher-order third term in eq 18 independently equal to zero gives

$$Q(s) = \theta(s) a l_B b^2 \mathbf{e} \tag{21}$$

Since $\theta(s)$ is less than its value in the polymer interior, we conclude that the condensed counterion layer is less stable on the end segment than in the interior. But a more interesting result emerges from a simple model in which the partition function $Q(s)$ is taken as the volume occupied by the condensed counterions. Then the local *concentration* of condensed counterions $\theta(s)/Q(s)$ is seen to equal a constant value throughout the end segment $s_0 < s < 1/\kappa$. As an example, this value, $1/a l_B b^2 \mathbf{e}$, is equal to 1.2 M for DNA (we take the salt as 1:1 and the bulk activity coefficient as unity). It is the same as the value of the local concentration in the interior of the polymer. In other words, the constant interior value of the local concentration of condensed counterions extends far into the Debye length end segment up to the "end effect length" s_0 before falling abruptly to zero. This behavior is definitely similar to that found by Washizu and Kikuchi,[27] who reported the surface concentration of counterions. With DNA parameters, they found that the surface concentration was slightly less than 2 M (it is expected to be somewhat higher than the local concentration of condensed counterions, not all of which are right at the surface of the polyion).

We are in a position at this point to estimate the electrostatic free energy density $g_{\text{el}}(s)$ as a function of length s along the end segment [$g_{\text{el}}(s)\,ds$ is the free energy in k_BT units associated with length interval ds]. In eq 12 the general term represents

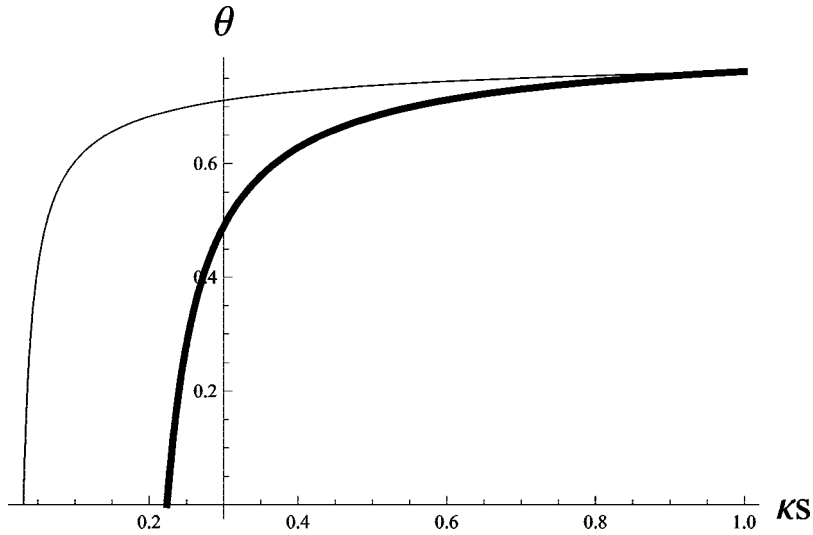

Figure 3. Condensed counterion fraction $\theta = z^{-1}(1 - f)$ on an end segment, as a function of reduced distance κs in from the end. Thick line: 0.1 M salt; thin line: 0.001 M salt. We have used univalent counterions, $z = 1$, and double-stranded DNA parameters in eq 19, $(\xi, b) = (4.2, 0.17\ \text{nm})$.

the Coulomb interaction between the mth site and a site that is n sites upstream from it (toward the interior). In view of the persistence of the constant internal value $1/z\xi$ of the effective charge fraction, we replace f_{m+n} by the constant $1/z\xi$. The upper limits of both sums are asymptotically equal to P. The double sum then separates, and when the outer sum is replaced by an integral, it becomes equal to $-\ln \kappa b$ (since $P \sim 1/\kappa b$). If the remaining summation over m is replaced by an integration over s, the Coulomb contribution to the electrostatic free energy density is easily identified (the number of charge sites in length ds is ds/b)

$$g_{\text{coulomb}}(s) = -\frac{1}{zb} f(s) \ln \kappa b \tag{22}$$

The contribution from the transfer free energy is straightforward

$$g_{\text{transfer}} = -\frac{1}{zb}[1 - f(s)] \ln(\mathbf{e}\kappa^2 b^2) \tag{23}$$

and then the overall free energy density is the sum of these two components

$$g_{\text{el}}(s) = -\frac{1}{zb}[(2 - f(s)) \ln(\kappa b) + 1 - f(s)] \tag{24}$$

To make effective use of this formula, it is convenient to refer it to the constant density $g_{\text{el}}(\infty)$ of the polymer interior. The latter is obtained by replacing $f(s)$ by its constant interior value $1/z\xi$. Then, defining $\Delta g_{\text{el}}(s) = g_{\text{el}}(s) - g_{\text{el}}(\infty)$, we have

$$\Delta g_{\text{el}}(s) = \frac{1}{zb}\left(\frac{1}{z\xi} - f(s)\right)(1 + \ln \kappa b) \tag{25}$$

In this formula, we remember that $f(s) = 0$ (no condensed counterions) in the interval $0 < s < s_0$, while it is given by eq 19 in $s_0 < s < \kappa^{-1}$. For DNA parameters, an integration from $s = 0$ to $s = 1/\kappa$ tells us that the electrostatic free energy of an end segment of length $1/\kappa$ at physiological ionic strength is 1.02 $k_B T$ units less than for an internal segment of the same length. The integration over the range $(0, s_0)$ accounts for about 70% of this amount. That is, most of the electrostatic stabilization is right at the end of the end segment and extends only slightly into the interior.

V. Junctions

The next construct we wish to study again consists of a set of discrete charge sites laid out on a straight line, which we regard as horizontal. From left to right, we number them as $-P_-, -P_- + 1, \ldots, -1, 0, 1, 2, \ldots, P_+$. There are also charge sites to the left of $-P_-$ and to the right of P_+. The uniform spacing between adjacent charge sites $(0, -1)$, $(-1, -2)$,... is b_-. The spacing between $(0, 1)$, $(1, 2)$,... is b_+. The spacing b_- is not equal to the spacing b_+, so that charge site 0 marks an interface between two polymer segments of different linear charge densities. The segment with negatively numbered sites we call $\mathscr{C}$. Segment $\mathscr{D}$ is the one with positively numbered sites. We refer to all sites within $\mathscr{C}$ and $\mathscr{D}$ as "the junction".

We take the lengths of segment $\mathscr{C}$, $(P_- - 1)b_-$, and of segment $\mathscr{D}$, $(P_+ - 1)b_+$, as both equal to $1/\kappa$. Charge interactions within the entire junction are taken as unscreened (they occur within a distance on the order of the Debye length). We regard interactions between the junction and the many sites both to its left and right as screened, and we neglect them.

The Coulomb free energy of the junction in $k_B T$ units may be written as

$$g_{\text{coulomb}} = \xi_- \sum_{n=1}^{P_-} \sum_{m=-P_-}^{-n} \frac{f_m f_{m+n}}{n} + \xi_+ \sum_{n=1}^{P_+} \sum_{m=0}^{P_+ - n} \frac{f_m f_{m+n}}{n} + l_B \sum_{-n \in \boldsymbol{C}} \sum_{m \in \boldsymbol{D}} \frac{f_{-n} f_m}{n b_- + m b_+} \tag{26}$$

In this formulation the first double sum represents Coulomb interactions within segment $\mathscr{C}$; the second double sum comes from the Coulomb interactions within segment $\mathscr{D}$; and the third double sum accounts for the "transjunction" interactions between pairs of sites, one in $\mathscr{C}$ and the other in $\mathscr{D}$. It is the interaction of segments $\mathscr{C}$ and $\mathscr{D}$ that distinguishes the junction from two isolated end segments, and the new technical difficulties encountered in analyzing the transjunction interaction must be surmounted.

We need $\partial g_{\text{coulomb}}/\partial \theta_l$, where, at first, site l is in segment $\mathscr{D}$

$$\frac{\partial g_{\text{coulomb}}}{\partial \theta_l} = -z\xi_+\left(f_{l-1} + \frac{1}{2} f_{l-2} + \cdots \frac{1}{l} f_0\right) - z\xi_+\left(f_{l+1} + \frac{1}{2} f_{l+2} + \cdots \frac{1}{P_+ - 1} f_{P_+}\right) - z l_B \left(\frac{f_{-1}}{l b_+ + b_-} + \frac{f_{-2}}{l b_+ + 2 b_-} + \cdots + \frac{f_{-P_-}}{l b_+ + P\_b_-}\right) \tag{27}$$

Of the three sums that appear, the first represents interactions of site l with sites in $\mathscr{D}$ closer to the interfacial site 0, including

the latter itself. We make no approximations in this sum. The second sum represents interactions of site l with sites in $\mathscr{D}$ further from the junction point. In this sum, we assume that the charge fractions f_{l+1},... have more or less reached a plateau value, and we replace all of them by f_l, which is then factored out, leaving a sum that we replace by an integral. The third sum represents interactions of site l with sites in segment $\mathscr{C}$. We separate this sum into its first $l-1$ terms and the remaining terms

$$-zl_B\left(\frac{f_{-1}}{lb_+ + b_-} + \frac{f_{-2}}{lb_+ + 2b_-} + \cdots + \frac{f_{-(l-1)}}{lb_+ + (l-1)b_-}\right)$$
$$-zl_B\left(\frac{f_{-l}}{lb_+ + lb_-} + \frac{f_{-(l+1)}}{lb_+ + (l+1)b_-} + \cdots + \frac{f_{-P_-}}{lb_+ + P_-b_-}\right)$$

The first of these sums represents interactions of site l in $\mathscr{D}$ with the first $l-1$ sites in $\mathscr{C}$. We make no approximations in this sum. The second sum represents interactions of site l with the more distant sites in segment $\mathscr{C}$. In this sum, we assume that the charge fractions $f_{-(l)}$, $f_{-(l+1)}$... have more or less reached a plateau value, and we replace all of them by f_{-l}, which is then factored out, leaving a sum that we replace by an integral. As in previous sections, we make the asymptotic approximation that fixed integers are negligible compared to P_- and P_+, and we recall the relation between the common length $1/\kappa$ of segments $\mathscr{C}$ and $\mathscr{D}$ and the number of sites P_- and P_+ in these segments.

In addition to $\partial g_{\text{coulomb}}/\theta_l$, we also need $\partial g_{\text{transfer}}/\theta_l$. From previous sections, we know that the dominant term in it is $-2 \ln \kappa b_+$. Then, since at equilibrium one of these derivatives must equal the negative of the other, we finally get the equilibrium condition

$$\xi_+ f_l \ln(\kappa \mathrm{b}_+) + \xi_- f_{-l} \ln[\kappa l(\mathrm{b}_+ + \mathrm{b}_-)] = \frac{2}{z}\ln(\kappa \mathrm{b}_+) + \xi_+\left(f_{l-1} + \frac{1}{2}f_{l-2} + \cdots + \frac{1}{l}f_0\right) + \xi_+\left[\frac{f_{-1}}{l + (b_-/b_+)} + \frac{f_{-2}}{l + 2(b_-/b_+)} + \cdots + \frac{f_{-(l-1)}}{l + (l-1)(b_-/b_+)}\right] \quad (28)$$

On the left of this equation stands two unknowns, f_l and f_{-l}. There is a symmetrical equation obtained from the equilibrium condition $\partial g_{\text{coulomb}}/\theta_{-l} = -\partial g_{\text{transfer}}/\theta_{-l}$. It reads

$$\xi_+ f_l \ln[\kappa l(\mathrm{b}_+ + \mathrm{b}_-)] + \xi_- f_{-l} \ln(\kappa b_-) = \frac{2}{z}\ln(\kappa \mathrm{b}_-) + \xi_-\left(f_{-l+1} + \frac{1}{2}f_{-l+2} + \cdots + \frac{1}{l}f_0\right) + \xi_-\left[\frac{f_1}{l + (b_+/b_-)} + \frac{f_2}{l + 2(b_+/b_-)} + \cdots + \frac{f_{l-1}}{l + (l-1)(b_+/b_-)}\right] \quad (29)$$

Equations 27 and 28 are a system of two linear equations in the two unknowns f_l and f_{-l}, but the "known" right-hand sides involve all the charge fractions at lower-number sites. These equations therefore provide an iterative scheme; if $f_0, f_{\pm 1}$,..., $f_{\pm(l-1)}$ have been determined, then f_l and f_{-l} can also be determined.

We can start by setting $l = 1$. Then f_1 and f_{-1} can be determined if f_0 is known. We can think of no a priori way of determining f_0, the charge fraction at the interface of segments $\mathscr{C}$ and $\mathscr{D}$. We proceed by imagining that the charge spacing b_0 in the immediate neighborhood of site 0 is an average, $b_0 = (1/2)(b_+ + b_-)$, and the charge fraction there is the corresponding average, $f_0 = 1/z\xi_0$, with $\xi_0 = l_B/b_0$. As an example, if segment $\mathscr{C}$ is a single helical strand of DNA, $\xi_- = 2.1$, and the corresponding value of $f_- = 1/(z\xi_-)$ far from the junction is 0.48 for univalent counterions. If segment $\mathscr{D}$ is double-helical DNA, $\xi_+ = 4.2$, and far from the junction the charge fraction $f_+ = 1/z\xi_+$ has the value 0.24. The value of the charge fraction f_0, calculated as above, then works out to be 0.36, which seems reasonable.

We show in Figure 4 the results of a calculation for univalent counterions at 0.01 M ionic strength, $\xi_- = 2.1$ for segment $\mathscr{C}$ (a helical single strand of DNA), and $\xi_+ = 4.2$ for segment $\mathscr{D}$ (double-helical DNA). Charge fraction is plotted against site number. The striking feature is that on both sides of the interface there is an immediate jump to plateau values that are not too different from the corresponding values for internal segments (0.48 for the single helix, 0.24 for the double helix). Once again, we see no correlation between the length $1/\kappa$ of the segments on either side of the junction interface and the distance from the interface at which the transition from low-density charge fraction to high-density charge fraction occurs.

As far as the electrostatic free energy is concerned, there is a cancelation effect, since the low-ξ side has lower free energy than the average, while the high-ξ side has a free energy higher

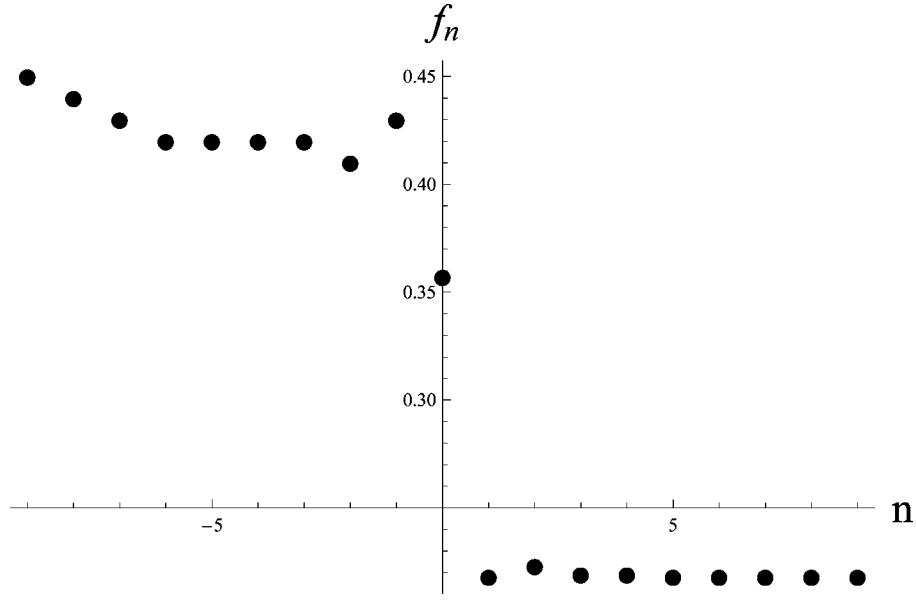

Figure 4. Charge fraction f_n at the nth site near a junction interface. The unit of length b_+ for sites to the right of the interface at the origin equals 0.17 nm ($\xi_+ = 4.2$) and to the left b_- =0.34 nm ($\xi_- = 2.1$). The 1:1 salt concentration equals 0.01 M, corresponding to $1/\kappa = 3.04$ nm.

than average. We have estimated the free energy density at the interfacial charge site 0 as differing from the average by less than 10% of a k_BT unit.

VI. End-On Approach of Rodlike Polyions

In this section we consider the interesting problem of how the potential of mean force between two identical rodlike polyions varies when the two polyions approach end-on. We specify the model clearly as follows. Choose a linear axis with ends at $\pm\infty$. Starting with a charge site numbered 1, place sites on this axis with uniform spacing b extending to $+\infty$, and number them 1, 2,..., $+\infty$. This set of charge sites represents one of the polyions. On the same linear axis, place charge sites extending to $-\infty$, also with uniform spacing b, and number them -1, -2,..., $-\infty$. This latter set of charge sites represents the other polyion. There is a gap between the two polyion ends, that is, between sites -1 and $+1$. For simplicity, the length of this gap is measured in multiples of b; say it equals wb. We will calculate the electrostatic free energy of this configuration for different fixed values of the positive integer w.

Although each polyion is semi-infinite, the only interactions we consider are within and between their respective Debye length end segments, $\mathcal{C} = (-P, -P+1,..., -1)$ and $\mathcal{D} = (1, 2,..., P)$, where $P - 1 = 1/\kappa b$. We take the Coulomb free energy as

$$g_{\text{coulomb}} = \xi\sum_{n=1}^{P-1}\sum_{m=-P}^{-n-1}\frac{f_m f_{m+n}}{n} + \xi\sum_{n=1}^{P-1}\sum_{m=1}^{P-n}\frac{f_m f_{m+n}}{n} + l_B e^{-(w-1)\kappa b}\sum_{-n\in C}\sum_{m\in D}\frac{f_{-n}f_m}{nb_- + mb_+} \quad (30)$$

where the first two double sums evaluate the respective Coulomb interactions within $\mathcal{C}$ and $\mathcal{D}$ and the third double sum is the interaction between charge sites in $\mathcal{C}$ and those in $\mathcal{D}$. Note that in the latter we have inserted a screening factor, which is essential, since we want our calculations to include large gaps when the two end segments are indeed screened from each other. The exponent has the factor $w - 1$ because when $w = 1$, the entire set of charge sites is indistinguishable from a single polyion with spacing b. We have chosen a common screening factor for all pair interactions between charge sites (one in $\mathcal{C}$ and one in $\mathcal{D}$) as a simplifying approximation (it accurately represents the screening of the charge pair $(-1, 1)$, where the largest effects will be found).

We need $\partial g_{\text{coulomb}}/\partial\theta_l$, and the procedure for calculating it is similar to the one used in the preceding section on junctions. An important difference is that after the differentiation of g_{coulomb} we may use the symmetry requirement $f_n = f_{-n}$ for all sites. Then the equilibrium condition $\partial g_{\text{coulomb}}/\partial\theta_l = -\partial g_{\text{transfer}}/\partial\theta_l$ (the transfer free energy is handled in the same way as for junctions) results in a single recursive relation for the single unknown f_l. The solution is

$$f_l = \frac{\frac{1}{z\xi}\ln P^2 - \sum_{n=1}^{l-1} f_{l-n}\left(\frac{1}{n} + \frac{1}{2l+w-2-n}e^{-(w-1)\kappa b}\right)}{e^{-(w-1)\kappa b}\ln\left[\frac{1}{2l+w-2}(P+l+w-2)\right] + \ln P} \quad (31)$$

$l = 1, 2,....$ The formula includes the charge fraction at site $l = 1$, since we understand that the summation in the numerator appears only for $l \geq 2$.

A few remarks are in order. The ln P terms incorporate the asymptotic approximations $P - i \sim P$ for fixed i that we have used throughout previous sections. The ln P term in the numerator originates from the local mixing contribution, and in the denominator it comes from part of the intrasegment interactions. The logarithmic term involving w is different. It contains information about the gap width, and we have not used the analogous approximation in writing it, since we do not want to wipe out the effect we are trying to estimate. The formula gives us f_l recursively for fixed gap width w; that is, to evaluate f_l, we first must have evaluated f_{l-1},..., f_1 for the same gap width. Notice that the result for f_1 with gap width $w = 1$, namely $f_1 = 1/z\xi$, is the exact result for the uniform charge fraction on an uninterrupted line of charges with spacing b. Finally, the formula also serves to evaluate the charge fractions on segment $\mathcal{C}$ through the symmetry condition $f_{-l} = f_l$.

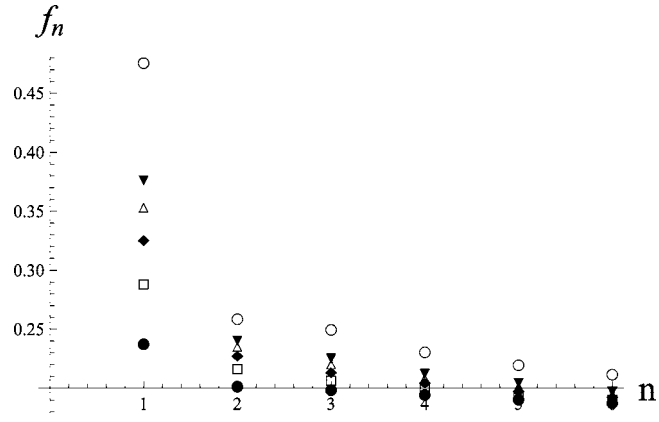

Figure 5. Charge fraction f_n at site number n on one side of a gap. The values are the same for the symmetrically positioned sites on the other side of the gap (not shown). At a given site number n on the horizontal axis, the gap width w increases from bottom to top: closed circle, $w = 1$ (no gap); square, $w = 2$; diamond, $w = 3$; up triangle, $w = 4$; down triangle, $w = 5$; open circle, $w = \infty$. 1:1 salt concentration, 0.05 M; $b = 0.17$ nm.

In Figure 5 we show the calculated charge fractions at charge sites $l = 1, 2,..., 6$ on segment $\mathcal{D}$. The same values hold for the corresponding negatively numbered sites on segment $\mathcal{C}$. At the 1:1 salt concentration used, 0.1 M, there are six sites in a Debye length segment with spacing b corresponding to double-helical DNA. At each charge site, from top to bottom, the distance wb between segments $\mathcal{C}$ and $\mathcal{D}$ (i.e., between sites ±1) decreases from infinity to b. At each site l, the charge fraction f_l is seen to decrease progressively as the segments approach each other. The transparent physical meaning is that counterion condensation increases at each site as the approach of the segments increases the charge density of the two-segment assembly of charges. The most important feature of Figure 5, however, is that this effect is large only for the end sites $l = \pm1$. The mutual approach of segments $\mathcal{C}$ and $\mathcal{D}$ has only a small effect on the charge fractions at sites $|l| \geq 2$.

Looked at conversely, as the segments move apart, counterions decondense from all sites but especially from sites ± 1, and the common charge fraction at these sites strongly increases. Figure 6 shows the increase of f_1 to a plateau value $2/z\xi$ as the segments move apart. The same observations hold true for the local partition functions Q_i, since each is proportional to the corresponding local value of the fraction of condensed counterions.

At infinite gap width, the charge fraction distribution on each segment should in principle be the same as for the end segment treated in section IV. The results differ, however, because the approximations used in the two calculations differ. The qualitative result of low counterion condensation at the end followed by a steep rise in condensation to a plateau well before the screening length is nonetheless the same in the two approaches, and both are consistent with the simulations of Washizu and Kikuchi[27] in this regard.

We turn to an estimate of the potential of mean force between segments $\mathcal{C}$ and $\mathcal{D}$. Since as these segments approach end-on

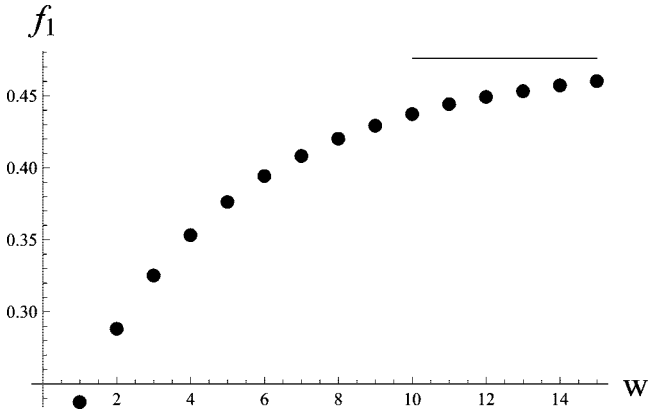

Figure 6. Charge fraction $f_{\pm 1}$ bordering the gap as a function of gap width. The horizontal line is the asymptote for infinite gap width. Parameters as in Figure 5.

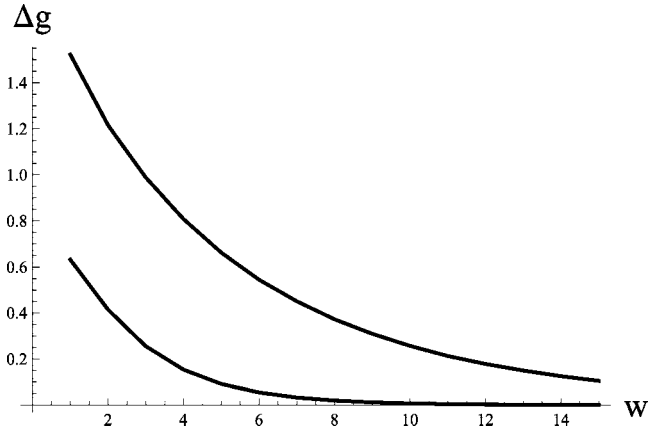

Figure 7. Potential of mean force Δg in k_BT units between two identical semi-infinite line charge segments as they approach end-on. The distance w between them is in units of $b = 0.17$ nm. Upper curve, 1:1 salt concentration, 0.05 M; lower curve, 1:1 salt concentration 0.5 M.

from infinity, the charge fractions do not change much for sites $|l| \geq 2$, we consider in eq 30 only those interactions involving the end sites ± 1, and we further approximate the charge fractions at all interior sites as equal to the polymer value $1/z\xi$ regardless of gap width w. Similarly, the local partition functions $Q_{\pm l}$ are assumed to be independent of gap width for $|l| \geq 2$, and in the mixing component of the electrostatic free energy only the terms involving $Q_{\pm 1}$ are considered. Finally, we recall the symmetry conditions $f_{-1} = f_1$ and $Q_{-1} = Q_1$. The resulting expression for $g_{el}(w)$ is ungainly but reasonably simple

$$g_{el}(w) = \frac{2}{z}\left\{f_1(w)e^{-(w-1)\kappa b}\ln\left(\frac{P+w-1}{w+1}\right) + [2-f_1(w)]\ln(P) - 1+f_1(w)\right\} + \frac{1}{w}\xi[f_1(w)]^2 e^{-(w-1)\kappa b} \quad (32)$$

where $f_1(w)$, the charge fraction at site 1 as a function of gap width w, is calculated from eq 31, and once more, the number of charges P in a Debye length segment equals $(1/\kappa b) + 1$. The potential of mean force $\Delta g_{el}(w)$ between segments $\mathcal{C}$ and $\mathcal{D}$ is then given by the difference $g_{el}(w) - g_{el}(\infty)$. Figure 7 exhibits plots of $\Delta g_{el}(w)$ for DNA parameters and two different salt concentrations. The curves have the appearance of typical repulsive potentials and are of the order of a k_BT unit at closest approach. The potential is strongly suppressed at high salt.

Kunze and Netz[28] have derived in elegant fashion a simple formula for the electrostatic closure free energy, that is, the work required to connect n charged rods of length L/n end-to-end to form a single rod of length L. Specialized to two rods, the formula accounts for the free energy over and above bending required to form a closed ring from a straight rod. The Kunze−Netz (KN) expression is derived in the Debye−Hückel approximation. In present notation, it reads (for two rods)

$$\Delta g_{\text{closure}} = \xi/\kappa b \quad (33)$$

in k_BT units. For DNA parameters ($\xi = 4.2$, $b = 0.17$ nm), the formula gives the huge values 33.5 and 10.6, respectively, at 1:1 salt concentrations 0.05 and 0.5 M. A rough way to modify these Debye−Hückel values to account for the presence of condensed counterions is to rescale the charge on each rod by the factor $1/\xi$. The corrected KN $\Delta g_{\text{closure}}$ then becomes equal to $1/(\xi\kappa b)$, yielding the much smaller values 1.9 and 0.6 k_BT units.

In our formulation of end-to-end approach, the closure free energy is given by the amplitude of the potential of mean force curve. For example, it follows from Figure 7 that the closure free energy is 1.5 k_BT at the lower ionic strength 0.05 M and 0.6 k_BT at 0.5 M. These values are close to the corrected KN values. The similarity of the two sets of values in this example is partly fortuitous. We have compared plots of corrected KN closure free energies with our present ones, and the curves by no means have the same shape (not shown). Moreover, the correction of the KN Debye−Hückel formula simply by a multiplicative charge renormalization factor is exceedingly rough, since proper inclusion of counterion condensation requires a calculation along the lines of what we have done in this paper (in other words, the whole subject of the present paper is the improvement of Debye−Hückel theory required when high charge densities cause nonlinear condensation of counterions). On the other hand, our own improvements on Debye−Hückel have come at the cost of many approximations, at least in the present case of nonuniform charge densities.

VII. A Possible Application to Cell Biophysics

In cell biology there is a class of proteins, called helicases, whose task it is to unwind the DNA double helix.[17] A helicase is a molecular motor that translocates along an unwound DNA strand, fueled by hydrolysis of nucleoside triphosphates like ATP. When it encounters the interface separating the two unwound strands from the remaining double helix, the helicase can wait passively for a thermal fluctuation to open the base pair ahead of it before proceeding into the fork, thus preventing reannealing of the base pair. Alternatively, the interaction of the helicase with the double helix may lower the free energy of a base pair opening fluctuation, thus actively facilitating entrance into the double helix. There are many different helicases, and some are thought to unwind the DNA "passively", while others unwind "actively".[18]

Johnson et al.[19] have performed an elegantly interpreted series of single-molecule kinetic experiments that provides evidence for active DNA unwinding by ring-shaped T7 helicase (a component of the T7 bacteriophage replication complex). To account for their kinetic data, these authors require an active destabilization interaction of $1-2$ k_BT per destabilized DNA base pair together with an interaction range ≥ 4 base pairs (and equal to 6 base pairs in an illustrative set of fitting parameters). For simplicity, the authors assumed a constant interaction energy over the range of the interaction.

The central channel of the ring-shaped helicase encloses a single DNA strand as it translocates along the strand. The central channel is lined with positively charged amino acids to accommodate the DNA phosphates inside it. In contrast, the exterior surface of the helicase is predominantly negatively charged. Johnson et al. suggest that the electrostatic repulsion between the exterior surface of the helicase and the negative

phosphate charge on the double helix may cause significant destabilization of the base pairs ahead of the approaching protein.

Given the complexity of the system, any attempt at a quantitative discussion based on coarse-grained models must be viewed cautiously; still, it seems worthwhile to estimate the expected magnitude of energetic effects predicted by simple electrostatic arguments. Recall, therefore, our calculation in the preceding section of the potential of mean force when the end segment of one polyion, say, segment $\mathscr{C}$, approaches another end segment $\mathscr{D}$. With DNA parameters, $\mathscr{D}$ can represent double-helical DNA at the fork. In the cell biology context, $\mathscr{D}$ is being approached, not by an identical double helical segment $\mathscr{C}$ but by the ring-shaped helicase bearing negative charge on its surface. Suppose, however, that the negative charge on the surface of the helicase is nature's way of replacing the negative DNA phosphate charge that the helicase disrupts and partially neutralizes as it progressively unwinds the two strands. In this spirit, the approaching segment $\mathscr{C}$ becomes a model for the electrostatic effect of helicase on the double-helical DNA (segment $\mathscr{D}$) in front of it. Figure 7 shows that the repulsive electrostatic interaction is about equal to 1.5 k_BT when segment $\mathscr{C}$ arrives at the edge of segment $\mathscr{D}$. The range of the repulsive potential shown in Figure 6 is 14 charge sites or 7 DNA base pairs.

In the set of fitting parameters used by Johnson et al. to illustrate their kinetic model, when the helicase is at the fork, it destabilizes 6 base pairs ahead of it by an amount 1.2 k_BT each, a total destabilization of 7.4 k_BT. The range of the repulsive potential in Figure 6 is similar to the range required by Johnson et al. Its amplitude, 1.5 k_BT, is about 20% of the needed amount. It should be noted that the ionic conditions used by Johnson et al. include Mg^{2+} ions, which are absent from our calculations. We can say little more on the basis of our fanciful model. Direct electrostatic repulsion between helicase and double-helical DNA may be less than or greater than our estimate of DNA−DNA repulsion. In this regard, the worth of our calculation may reside in its demonstration that in principle electrostatic destabilization of double-helical DNA may be a component of the active unwinding mechanism of ring-shaped helicase, as suggested by Johnson et al.

There is, however, another aspect to the electrostatics of the helicase−DNA interaction that we may be able to model more realistically. The helicase approaches the fork along one of the DNA single strands protruding from the fork. The other single DNA strand is displaced by the protein. Johnson et al. suggest that the displaced single strand can mediate a destabilization mechanism supplementing electrostatic repulsion from the negatively charged helicase surface. They point out that the displaced DNA single strand must be bent away from the fork and the central channel of the helicase and that the persistence length of the single strand is sufficient to transmit elastic bending stress to the interface with the intact double helix at the fork. But in addition to the elastic stress, the bent-back single strand would also position more phosphates in the vicinity of the double helix at the fork. The additional negative charge density from the bent-back single strand would destabilize the intact base pairs at the fork.

Consider an extreme model in which the bent-back single strand is sterically forced to lie along the DNA double helix at the fork for a distance of a few intact base pairs. Suppose the effect is that each base pair in this environment effectively "owns" three phosphate groups instead of two. We can estimate the destabilizing free energy increment Δg due to this additional electrostatic stress, per base pair, as $3g(\xi_3) - 2g(\xi_2)$, where $g(\xi)$ is electrostatic free energy in k_BT units per charge site for a line of charge sites with charge density parameter ξ (and spacing b).[5,6] For double-helical DNA with its usual quota of two phosphates per base pair, $(\xi_2, b_2) = (4.2, 0.17\ \text{nm})$, and for a double-helical DNA loaded with an additional phosphate per base pair, $(\xi_3, b_3) = (6.3, 0.11\ \text{nm})$. We then calculate from[5,6]

$$g(\xi) = -\frac{1}{z}\left(2 - \frac{1}{z\xi}\right)\ln(1 - e^{\kappa b}) - \frac{1}{z} + \frac{1}{z^2\xi} \tag{34}$$

that $\Delta g = 5.4\ k_BT$ per base pair ($z = 1$, 0.05 M 1:1 salt), or about 4−5 times more than the 1.2 k_BT needed by Johnson et al. to account for their data, leaving some room for modeling inaccuracies.

VIII. Summary

We have given approximate solutions for the effective charges and electrostatic free energies of several constructs involving nonuniform distributions of the bare charges. Specifically, we have treated line-charge models for oligoelectrolytes, end segments, junctions, and the end-on approach of two rodlike polymers. A theme that pervades the results is that the Debye screening length does not appear to be the appropriate length scale for measuring how the local number of condensed counterions tracks the nonuniformities. We find a significant condensation on oligomers shorter than the screening length. Additionally, the uniform condensation charge density in the interior of a long polymer extends nearly to the physical ends of the polymer, penetrating far into Debye length segments at the ends. At a junction where two distributions of bare charges with uniform but differing charge densities meet, the width of the transition of the local condensation fraction is much less than a Debye length. These results are perhaps not so unexpected in view of the fact that the screening length is a concept originating in linear theory, whereas counterion condensation reflects a nonlinear response.

We cannot rule out the possibility that our analytical results are biased by the approximations used to obtain them. We are encouraged to believe that the approximations are realistic by the consistency of their consequences with the simulated data of Washizu and Kikuchi for polymer ends[27] and of Netz[25] and Frank and Winkler[26] for oligomers.

Acknowledgment. The author acknowledges informative discussions and correspondence with Roland G. Winkler and Michelle D. Wang.

References and Notes

(1) Manning, G. S. *Q. Rev. Biophys.* **1978**, *11*, 179.
(2) Manning, G. S. *Acc. Chem. Res.* **1979**, *12*, 443.
(3) Manning, G. S. *J. Phys. Chem.* **1981**, *85*, 1506.
(4) Manning, G. S. *Ber. Bunsenges. Phys. Chem.* **1996**, *100*, 909.
(5) Manning, G. S. *Macromolecules* **2001**, *34*, 4650.
(6) Manning, G. S. *Biophys. Chem.* **2002**, *101*−*102*, 461.
(7) Keyser, U. F.; Koeleman, B. N.; van Dorp, S.; Krapf, D.; Smeets, R. M. M.; Lemay, S. G.; Dekker, N. H.; Dekker, C. *Nat. Phys.* **2006**, *2*, 473.
(8) Magdelenat, H.; Turq, P.; Tivant, P.; Menez, R.; Chemla, M.; Drifford, M. *Biopolymers* **1979**, *18*, 187.
(9) Blaul, J.; Wittermann, M.; Ballauf, M.; Rehahn, M. *J. Phys. Chem. B* **2000**, *104*, 7077.
(10) Essafi, W.; Lafuma, F.; Williams, C. E. *Eur. Phys. J. B* **1999**, *9*, 261.
(11) Essafi, W.; Lafuma, F.; Baigl, D.; Williams, C. E. *Europhys. Lett.* **2005**, *71*, 938.
(12) Kakehashi, R.; Maeda, H. *J. Chem. Soc., Faraday Trans.* **1996**, *92*, 3117.
(13) Kakehashi, R.; Maeda, H. *J. Chem. Soc., Faraday Trans.* **1996**, *92*, 4441.
(14) Kozak, D.; Dolar, D. *Z. Phys. Chem. (Frankfurt)* **1971**, *76*, 93.
(15) Reddy, M.; Marinsky, J. A. *J. Phys. Chem.* **1970**, *74*, 3891.
(16) Oman, S.; Dolar, D. *Z. Phys. Chem. (Frankfurt)* **1967**, *56*, 13.
(17) Alberts, B.; Johnson, A.; Lewis, J.; Raff, M.; Roberts, K.; Walter, P. *Molecular Biology of the Cell*, 5th ed.; Garland Science: New York, 2007.

(18) Lohman, T. M.; Bjornson, K. P. *Annu. Rev. Biochem.* **1996**, *65*, 169.
(19) Johnson, D. S.; Bai, L.; Smith, B. Y.; Patel, S. S.; Wang, M. D. *Cell* **2007**, *129*, 1299.
(20) Olmsted, M. C.; Anderson, C. F.; Record, M. T. *Proc. Natl. Acad. Sci. U.S.A.* **1989**, *86*, 7766.
(21) Ramanathan, G. V.; Woodbury, C. P. *J. Chem. Phys.* **1982**, *77*, 4133.
(22) Katoh, T.; Ohtsuki, T. *J. Polym. Sci., Polym. Phys.* **1982**, *20*, 2167.
(23) Odijk, T. *Physica A* **1991**, *176*, 201.
(24) Manning, G. S.; Mohanty, U. *Physica A* **1997**, *247*, 196.
(25) Netz, R. R. *J. Phys. Chem. B* **2003**, *107*, 8208.
(26) Frank, S.; Winkler, R. G., submitted for publication.
(27) Washizu, H.; Kikuchi, K. *J. Phys. Chem. B* **2006**, *110*, 2855.
(28) Kunze, K. K.; Netz, R. R. *Phys. Rev. E* **2002**, *66*, 011918.
(29) Cottet, H.; Gareil, P.; Theodoly, O.; Williams, C. E. *Electrophoresis* **2000**, *21*, 3529.

MA800628V